ACS Macro Letters
Viewpoint
pubs.acs.org/macroletters

High χ–Low N Block Polymers: How Far Can We Go?

Christophe Sinturel,*[†,‡] Frank S. Bates,*[§] and Marc A. Hillmyer*[‡]

[†]ICMN, UMR 7374 - CNRS/Université d'Orléans, 1b rue de la Férollerie, 45071 Orléans, France

[‡]Department of Chemistry and [§]Department of Chemical Engineering and Materials Science, University of Minnesota, Minneapolis, Minnesota 55455-0431, United States

ABSTRACT: Block polymers incorporating highly incompatible segments are termed "high χ" polymers, where χ is the Flory–Huggins interaction parameter. These materials have attracted a great deal of interest because low molar mass versions allow for the formation of microphase-separated domains with very small (<10 nm) feature sizes useful for nanopatterning at these extreme dimensions. Given that well-established photolithographic techniques now face difficult challenges of implementation at scales of 10 nm and below, the drive to further develop high χ block polymers is motivated by trends in the microelectronics industry. This Viewpoint highlights our perspective on this niche of block polymer self-assembly. We first briefly review the relevant recent literature, exploring the various block polymer compositions that have been specifically designed for small feature size patterning. We then overview the now standard method for the benchmarking χ values between different pairs of polymers and the consequences of low N and high χ on the thermodynamic aspects of microphase separation. Finally, we comment on restrictions going forward and offer our perspective on the future of this exciting area of block polymer self-assembly.

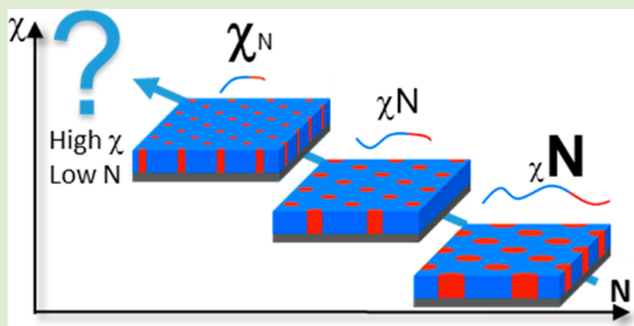

To support the ever growing microelectronics industry, manufacturing techniques have advanced to the point where the dimensions of the elementary engineered features have reached the 10 nm length scale.[1] Miniaturization of transistor sizes and concomitant increases in on-chip density has fed the constant need for smaller devices with increased processing speed and storage capacity. To achieve such miniaturization, photolithography has been the workhorse of the industry over the past decades. However, the drive to even smaller nanostructures and higher densities has thwarted even the most advanced photolithography, and further evolution of these techniques for routine generation of sub-10 nm features faces significant challenges.

Materials that spontaneously self-assemble to form discrete nanostructures have emerged as promising solutions to this dilemma because extremely small feature sizes can be readily and reproducibly generated in thin films over large areas. Block polymers in particular can adopt ordered and oriented nanopatterns on surfaces that can be subsequently transferred to the underlying substrate with high fidelity. In fact, block polymer based nanopatterning techniques have been highlighted as key future technologies on the International Technology Roadmap for Semiconductors (ITRS).[2] Advances in polymer synthesis, control of nanopattern orientation/alignment, and processing methods have allowed the creation of functional electronic devices with areal densities that go well beyond current photolithographic limits; several comprehensive reviews documenting these successes have recently appeared.[3−8]

The thermodynamic driving force that leads to segregation of the two (or more) chemically disparate polymer blocks lies at the heart of self-assembly on the scale of the natural dimensions of the component macromolecules. At equilibrium, the ordered state symmetry and sizes of the structures that emerge from the self-assembly process are largely governed by the volume fraction of each block (composition, f_i) and the overall degree of polymerization N of the block polymer (proportional to the molar mass). However, sufficient incompatibility between the constituent monomers is required for self-assembly. Following the spirit of most modern interpretations of Flory–Huggins theory,[9] it is convenient to combine all excess thermodynamic contributions to the overall free energy (i.e., enthalpic and noncombinatorial entropic factors) into an effective interaction parameter denoted χ_{eff}. (Here we note that χ and χ_{eff} are used interchangeably in this Viewpoint.) Mean-field theory predicts that symmetric AB diblock copolymers ($f_A = 1 - f_B = 1/2$) will produce ordered structures when the product $\chi_{eff}N$ (using a value of N based on a common segment reference volume, $\nu_A = \nu_B$) is greater than 10.5.[10,11] Thus, at fixed χ_{eff}, there is a minimum value of N necessary for self-assembly. In general terms, values of N below this limit give disordered structures that have little value for nanopatterning. Given that the dimensions of the self-assembled structures that result from block polymer ordering are sensibly related to the overall size of

Received: July 10, 2015
Accepted: August 25, 2015
Published: September 2, 2015

ACS Publications © 2015 American Chemical Society

DOI: 10.1021/acsmacrolett.5b00472
ACS Macro Lett. 2015, 4, 1044−1050

the component macromolecules, higher values of χ_{eff} allow for lower values of N and thus smaller features. For illustrative purposes (only), strong segregation theory predicts that the lamellar domain spacing $d \approx bN^{2/3}\chi_{eff}^{1/6}$, where b is the statistical segment length.[12] (The term L_0, known as the pitch, is commonly used in the lithography literature rather than d.) Applying $(\chi_{eff}N)_{ODT}$ = 10.5 and a maximum value for b for flexible polymers of about 1 nm leads to $d \geq 5\chi_{eff}^{-1/2}$ nm. Under these simplifying assumptions, domain feature sizes (d/2) in lamellar forming block polymers can, in principle, be as low as 8, 5, and 2.5 nm at χ_{eff} values of 0.10, 0.25, and 1.0, respectively (at corresponding minimum values of N = 105, 42, and 11, respectively). Thus, the drive to high χ (or, more generally, χ_{eff})−low N block polymers is motivated by the allure of generating sub-10 nm nanopatterns.

This Viewpoint highlights our perspective on this particular niche of block polymer science and engineering. We first briefly highlight examples of high χ−low N block polymers in the literature, emphasizing important recent contributions that have been specifically designed for patterning of small feature sizes. We then overview a now standard practical method for the benchmarking of χ_{eff} and the consequences of high χ and low N on the thermodynamic aspects of self-assembly. Finally, we give our views on how far we think this downscaling can go and comment on intrinsic restrictions in this low feature size limit.

■ INTRODUCTION AND BACKGROUND

In early experimental reports highlighting the beneficial use of block polymers with increased incompatibility in self-assembled thins film for nanopatterning purposes, improved long-range order and reduced line edge roughness were the main focal points.[13] Systems, such as poly(styrene)-*b*-poly(ethylene oxide) (PS−PEO)[14] and PS-*b*-polydimethylsiloxane(PDMS),[15] characterized by enhanced incompatibility relative to the industry standard PS-poly(methyl methacrylate) [PMMA], favor long-range ordering[16] and sharper interfaces, which may translate into reduced line edge roughness. (Whether these effects actually provide practical benefits in the thin film limit, where competing wetting interactions with the film boundaries may dominate, remains an open question). The notion of using high χ materials to enable the use of low N materials for the realization of smaller domain sizes and, thus, higher areal feature densities was explicitly stated in a paper published in 2007 by Cavicchi et al.[17] However, the poly(isoprene)-*b*-poly(lactide) (PI-PLA) studied in that work was selected primarily for facile domain orientation by solvent annealing. One early example demonstrating reduction in domain size originating from enhanced incompatibility between chain segments was published in 2008 by Park et al., in hybrid systems combining block polymers and inorganic species.[18] They achieved 7 nm half-pitch line patterns using low molar mass PS-PEO (5 kg mol^{-1}) blended with organosilicate oligomers. Other early examples demonstrating enhanced incompatibility between chain segments with selective addition of lithium salts in PEO-based block polymers and the associated reduction in domain size[19,20] helped motivate a 2009 work describing the incorporation of a metal salt in PS-PEO resulting in PEO domains as small as 3 nm.[21] While this certainly is a viable approach, incorporation of metal salts in block polymer thin films can compromise subsequent processing steps and device applications. Here we focus our attention on pristine organic, or silicon-containing, block polymers with high degrees of incompatibility.

Attempts to prepare block polymers with intrinsically large interaction parameters began in earnest earlier this decade, and silicon-containing block polymers received a good deal of interest in this regard. As an added benefit, such systems possess natural contrast for facile pattern transfer to the substrate upon oxygen plasma etching.[22] PDMS-containing block polymers, where the Si−O bonds constitute the backbone of the polymer, were the first candidates used for this purpose.[23] In 2010, Jung et al. reported the formation of arrays of parallel cylinders with 17 nm periods and 8 nm line widths, using a PS-PDMS sample with an overall molar mass of 16 kg mol^{-1}.[24] PDMS was used in combination with poly(2-vinylpyridine) [P2VP] to form 6 nm cylinders[25] and with PMMA to form a lamellar morphology with a period of about 12 nm in thin films.[26] In the latter case, block polymers with molar masses as small as 3.9 kg mol^{-1} still exhibited microphase separation at room temperature. PDMS in combination with PLA allowed for further enhanced incompatibility between the blocks. The Flory−Huggins interaction parameter reported for this combination by Rodwogin et al. was estimated to be close to unity at 150 °C and is one of the largest reported to date,[27] enabling the formation of exceptionally small domains. They argue that this system has the capability of producing lamellar phases with PLA and PDMS domains about 3.5 nm in width. Cylindrical and spherical morphologies, with diameters around 10 nm, were also successfully prepared using closely related block polymers.[28]

Another family of silicon-containing block polymers places the Si atoms pendant to the backbone, including PS-*b*-poly(trimethylsilylstyrene) [PTMSS], PS-*b*-poly(pentamethyldisilylstyrene) [PPDSS], poly(4-methoxystyrene-*b*-PTMSS) [PMOST-*b*-PTMSS], and PS-*b*-methyltrimethylsilyl methacrylate) [PTMSM].[29−31] These compounds generated lamellar morphologies at sub-20 nm length scales, with good control over domain orientation through directed self-assembly and top coating techniques.[32] Using PTMSS tethered to PLA[33] or oligosaccharides, Cushen et al. reported features as small as 5 nm in a cylindrical forming block polymer in the latter case (see Figure 1).[34]

Fully organic (i.e., sans metals or Si) block polymers also have garnered significant interest since they too can afford

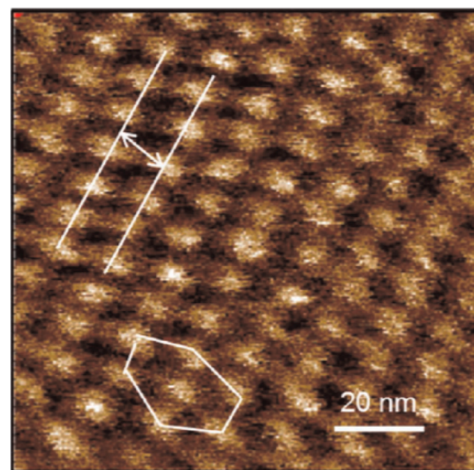

Figure 1. AFM phase image of a thin film of maltoheptaose-*block*-poly(trimethylsilylstyrene), showing 5 nm self-assembled features where the interplanar distance (arrow) is 11.4 nm. Reproduced with permission from ref 34. Copyright 2014 American Chemical Society.

DOI: 10.1021/acsmacrolett.5b00472
ACS Macro Lett. 2015, 4, 1044−1050

access to sub-10 nm features. Sugar-based polymers, like rod–coil amylose-*b*-PS, as reported by Aissou et al., were demonstrated to be very effective in producing small feature sizes using low molar mass compounds.[35] Taking advantage of the strong mutual repulsion between the hydrophilic sugar moiety and the hydrophobic PS block, domains on the order of 10 nm were observed for block polymers with as few as 40 repeat units. Poly(4-vinylpyridine) [P4VP] also is highly incompatible with hydrophobic blocks due to the strong polarizability of the pyridine ring.[36] This was exploited in a symmetric PS-P4VP block copolymer where fingerprint patterns with sub-12 nm characteristic length scales were achieved.[37] Block polymers containing PS derivatives with increased hydrophobicity such as poly(4-*t*-butylstyrene) (PtBS) and poly(cyclohexylethylene) (PCHE) were successfully used to achieve high levels of block incompatibility. For example, 14 nm lamellae periods were reported by Kennemur et al. using PtBS-poly(methyl methacrylate) [PMMA].[38] Similarly, Sweat et al. generated lamellae and cylinders from PtBS-P2VP with minimum full pitch of 10 and 6 nm, respectively.[39] Very recently, Kennemur et al. reported the synthesis of low molar mass PCHE-*b*-PMMA samples with sub-5 nm nanodomains.[40] The ultrasmall feature sizes associated with this material were achieved at N = 64, consistent with the simple strong segregation estimates presented above.

We catalogue the characteristic length scales produced by a host of block polymer systems to illustrate the evolution of the feature sizes achieved over the last two decades in Table 1. The constant downscaling, from L_0 > 20 nm in the case of the canonical systems (e.g., PS–PMMA) to sub-10 and now sub-5 nm domain dimensions (half-pitch) has been made possible by the formation of low molar mass compounds that remain microphase-separated at requisite processing temperatures due to the high level of incompatibility. Table 1 also provides estimates of the effective Flory–Huggins parameters (χ_{eff}), scaled to a common statistical segment volume (v = 0.118 nm^3), based on information provided by the authors of these studies.

Table 1. Characteristic Dimensions and χ Coefficient for a Variety of Block Polymers[a]

block polymer	M_n (kg mol^{-1})	morphology	characteristic dimensions (nm)	χ_{eff} 150 °C (and method of estimation)
MH-PTMSS	3.9	Hex	D = 5.5, d = 8.3[34]	not known
P2VP-PDMS	26.0	Hex	D = 6, L_0 = 26[25]	not known
PTMSS-PLA	9.2	Hex	D = 8.8, d = 12.1[33]	0.41[33] (SAXS)
PS-PDMS	16.0	Hex	D = 8, L_0 = 20[45]	0.11[46,40] (ODT)
PS-PLA	18	Hex	D = 10, L_0 = 18[47]	0.075[48] (ODT)
Mal-PS	4.5	Hex	D = 12[35]	not known
PDMS-PLA	9	Hex	D = 13, d = 20[28]	1.1[27] (domain spacing)
PS-PMMA	42	Hex	D = 14, L_0 = 24[49]	0.030[50] (SANS)
PS-PEO	21	Hex	D = 17.4[51]	0.047[52] (SAXS)
PCHE-PMMA	4.9	Lam	L_0 = 9.0[40]	0.18[40] (ODT)
PtBS-PVP	4.5	Lam	L_0 = 9.6[39]	0.11[39] (ODT)
PS-P4VP	6.4	Lam	L_0 = 10.3[37]	0.40[36] (SAXS)
PtBS-*b*-PMMA	17.6	Lam	L_0 = 14.4[38]	0.053[38] (ODT)
PMOST-PTMSS	8.5	Lam	L_0 = 14.4[30]	0.046[30] (ODT, SAXS)
PS-PDMS	16.0	Lam	L_0 = 17.5[24]	0.11[46,40] (ODT)

[a]For the hexagonally packed cylindrical morphology (Hex): L_0 is the center-to-center spacing, d is the 100 interplanar distance of the hexagonal lattice, D is the diameter of the cylinder. For the lamellar morphology (Lam): L_0 is the domain spacing, also referred in the lithography oriented literature as "pitch", the width of the lamellae (or "half-pitch") is given by $L_0/2$. All the values of χ are scaled to a common reference volume of 0.118 nm^3. Method of estimation of χ_{eff}: determined by random phase approximation (RPA) using absolute intensity SAXS (or SANS) vs temperature in the disordered state (denoted SAXS or SANS); determined by mean-field theory using ODT (denoted ODT); determined using strong segregation theory and the domain spacing (denoted domain spacing).

■ ORDER AND DISORDER: THEORY VERSUS PRACTICE

Implementing the myriad versatile synthetic approaches available for producing high χ (low N) block polymers is inextricably coupled to the methods associated with experimentally qualifying and theoretically anticipating the products. While the general principles that govern block polymer phase behavior are well-established, none of the current theories that model the ordered state morphologies, molecular factors that determine the location of the order–disorder transition, or underlying segment–segment interaction parameters, are sufficiently predictive to be used a priori in designing new materials. Nevertheless, guided by theory, the judicious application of targeted synthesis and morphological characterization provides an efficient strategy for the development of new block combinations and predictive design parameters.

Modern block copolymer theory originated in the 1970s with the seminal work of Helfand and co-workers,[41−43] where the interfacial composition profile in a microphase separated diblock copolymer, $\rho_A = 1/2[1 - \tanh(2x/a_I)]$, was shown to be governed by the magnitude of χ, where $a_I = (2/6^{1/2})b\chi^{-1/2}$ represents the interfacial width. In 1980, Leibler published a landmark paper that applied self-consistent mean-field theory (SCFT), based on the random phase approximation (RPA), to predicting the universal phase behavior of diblock copolymers in terms of the combination parameter χN and the molecular composition $f_A = N_A/(N_A + N_B)$, where $v_A = v_B$.[10] Importantly, this theory, which is rigorously correct only in the limit $N \to \infty$, anticipates weak block segregation and, thus, broad interfacial widths near the order–disorder transition, $(\chi N)_{\text{ODT}}$ = 10.5 when f_A = 1/2, resulting in $d \sim N^{1/2}$. Transition to strong segregation, as mentioned above, and $d \sim N^{2/3}$ occurs when $\chi N \gg 10$. Subsequent work by Fredrickson and Helfand corrected the SCFT theory for the effects of composition fluctuations at finite N, added a $N^{1/3}$ dependence to $(\chi N)_{\text{ODT}}$, and changed the character of the ODT to weakly first-order.[44]

Unfortunately, this fluctuation correction becomes unphysical in the limit of small N, where the amplitude of the compositional profiles approach the limit of strong segregation, even in the disordered state, as recently shown by Morse and co-workers.[53,54] Molecular simulations indicate that for N < 100, $(\chi N)_{\text{ODT}}$ > 20, introducing significant uncertainty in the

DOI: 10.1021/acsmacrolett.5b00472
ACS Macro Lett. 2015, 4, 1044−1050

ability to quantitatively predict the molar mass required to achieve a specific thermodynamic state. On the other hand, increasing χ and correspondingly decreasing N also leads to strong segregation (i.e., large values of χN) and well-formed microdomains all the way down to T_{ODT} (enabling the use of the simple predictive tools summarized in the introduction)[12] and offering the possibility of preparing viable lithographic materials with optimally reduced pitch and relatively discrete interfaces even near the disordering transition. Moreover, fluctuation effects do not appear to compromise pattern formation in the thin film limit.[55] However, recent work with PS-PMMA suggests that additional factors may compromise satisfactory pattern transfer as $\chi N \rightarrow (\chi N)_{ODT}$.[56]

For nanopatterning purposes block polymer thin films should be in an ordered state at a processing temperature higher than the highest glass transition (or melting) temperature of the constituent blocks. That is, the thin film sample should be in an organized (and ideally aligned, with an ultralow defect density) state prior to vitrification of the material upon cooling, which renders the film mechanically robust and suitable for pattern transfer operations. Films are then generally annealed at temperatures allowing enough polymer mobility to facilitate any inherent order−order transitions. Of course, film formation and subsequent processing temperatures should be below the point of decomposition (e.g., cross-linking, chain degradation) of the block polymer. Thus, the lithographic agent must be strategically designed with respect to molar mass to juxtapose processing conditions such as thermal or solvent annealing and the order−disorder transition temperature. High defect density may be an issue for these low N materials since defects like dislocations and disclinations become thermodynamically more favorable in such case, which can compromise pattern integrity and reduce T_{ODT}.[57] However, the ability to anneal away defects and self-direct assembly on surface patterns also becomes more facile near the ODT since the barrier associated with defect annihilation becomes $\ll k_BT$.[58,59] (Solvent annealing has also been shown to be associated with bringing ordered thin films close to this condition[47,60] due to the decrease in χ associated with the dilution effect.[61,62]) In addition, increasing χ (and reducing N) strengthens the first-order character of the transition, enabling the simultaneous reduction in domain size while minimizing defect density using processing techniques. Correlation of χ and N (rather than an overall χN value) to the defect density is, however, still an open question since simultaneous variation in chain length (N) and χ while maintaining a constant χN product produces significantly different defect-free energies.[63]

We and others have developed a straightforward approach to generating the required design parameters. Making the simplifying assumptions that $(\chi_{eff}N)_{ODT} = 10.5$ and $\chi_{eff} = \alpha T^{-1} + \beta$ permits the determination of the system dependent coefficients α and β based on the analysis of a few symmetric diblock copolymers. An important feature of this approach is specification of a common segment volume, v_0, based on measured or estimated polymer densities, which then defines N for a particular molar mass (see Table 1). This use of common segment volume is consistent with lattice nature of the original Flory−Huggins theory. The magnitude of χ_{eff} can be first estimated based on crude but efficient techniques such as solubility parameters or group contribution approaches leading to the synthesis of a symmetric diblock with a targeted T_{ODT} between the highest melting or glass transition temperature (T_{min}) and the chemical decomposition temperature (T_{max}, typically greater than 300 °C). For most polymer pairs, a T_{ODT} of 150 °C (423 K) would comfortably fall within this range. Well established methods, including dynamic mechanical spectroscopy (DMS)[64] and small-angle X-ray[65] or neutron scattering[50] (SAXS, SANS), are then employed to determine the actual T_{ODT}. An added dividend when working with low N block polymers is the ability to identify T_{ODT} by differential scanning calorimetry (DSC), made possible by the proportional increase in the heat of transition that accompanies larger χ_{eff} parameters.[66−69] The main issue is determining what block polymer molar mass will give a T_{ODT} of 150 °C. Of course, this depends on the value of χ_{eff} at 150 °C; for example, if χ_{eff} is 0.2 at 150 °C, the targeted N should be about 50. At $\chi_{eff} = 0.02$, the targeted N should be about 500. This range of χ values at 150 °C spans from one of the most highly incompatible organic diblock polymers demonstrated to date (PCHE-PMMA) to one of the most-utilized, but relatively weakly segregated (PS-PMMA). For other representative compounds in the literature, an ODT at 150 °C would require the values of N (using the typically employed reference volume, v_o, of 0.118 nm^3) for PS-PEO, PS-PI, and PS-PDMS of about 225, 150, and 100, respectively.

As a specific example, suppose the diblock copolymer under consideration is PS-PLA. Based on solubility parameters, the estimated incompatibility between these two polymers is between PS-PI and PS-PDMS, so 120 would be a reasonable target value for N. In a symmetric sample with $N_{PS} = 60$ and $N_{PLA} = 60$, each block will have a volume of 60×0.118 nm^3 = 7.1 nm^3, and a mole of either block would occupy about 4300 cm^3. Using a density for PS of 1 and 1.2 g/cm^3 for PLA dictates PS and PLA blocks of about 4.3 and 5.2 kg/mol, respectively, for an overall molar mass of approximately 10 kg/mol. In fact, a sample very near this value has $T_{ODT} = 116$ °C.[48] As a rule of thumb, in this high χ regime, changing the molar mass by about 20% will give an ODT that is well removed from the original value, but will allow experimental observation of another T_{ODT} within the typical range $T_{min} < T_{ODT} < T_{max}$. Whether the molar mass of the second sample is increased or decreased from the original sample will depend on the proximity of T_{ODT} for the first sample to T_{min} or T_{max}. In this particular example, the proximity of 116 °C to the glass transition temperature of PS (≈100 °C) suggests increasing N to 144 or to a molar mass of about 12 kg/mol; in fact, such a symmetric PS-PLA diblock exhibits an ODT temperature of 164 °C.[48] With these two ODT temperatures and the associated N, two values of $\chi_{eff}(T)$ can be calculated: 10.5/120 = 0.088 at 116 °C (389 K) and 10.5/144 = 0.073 at 164 °C (437 K), leading to $\chi = 53T^{-1} - 0.05$, in relatively close agreement with the published values α = 57.4 and β = 0.06.[48] Preparation and evaluation of additional diblock copolymer specimens with different values of N provides for tighter statistical significance in α and β. While not rigorously correct, this approach leads to a practical working relationship for $\chi_{eff}(T)$ that provides surprisingly precise conditions for molar mass to place T_{ODT} at a specified value[38] even in the limit of sub-5 nm domain dimensions.[40] This method has been successfully applied to several other systems.[30,38,40]

■ PERSPECTIVE GOING FORWARD

How far down in N (hence, d or L_0) can the approaches outlined here be pushed in practice? Does $N \rightarrow 1$ translate to $\chi_{eff} \rightarrow 10.5$? Of course, in this limit, the molecules are no longer polymers and extension of the concepts associated with block

DOI: 10.1021/acsmacrolett.5b00472
ACS Macro Lett. 2015, 4, 1044−1050

polymer theory clearly will fail. The work cited in this perspective demonstrates that the crude application of the mean-field theory (strictly rigorous only in the limit $N \to \infty$) based on an effective interaction parameter is surprisingly applicable at values of N as low as 20 and perhaps even 10, with domain sizes approaching 2 nm with flexible polymer blocks. Combining fluorinated monomers with strongly polar repeat units, perhaps containing ionic moieties, opens the door to the thermotropic ordering of amphiphilic molecules where $N \to 1$.[70,71] Such small molar masses transform what we consider to be block polymers into what is more appropriately referred to as liquid crystals, where $d \sim N$ and the notion of a simple (scalar) segment−segment interaction parameter must be replaced by more detailed structural features including nematic and smectic order parameters and more complex (e.g., Maier−Saupe type) intermolecular interactions.[72] Recent work with this class of liquid crystalline ordering suggests the possibility of long-ranged pattern formation with ∼1 nm resolution.[73] In our opinion, the application of "high χ−low N" block polymers will allow the formation of well-defined features as small as 2 nm.

The synthesis of block polymers at such low molar masses is actually technically quite straightforward in many ways. When using controlled polymerization techniques, large quantities of initiator allow for a higher tolerance of impurities. Reaction rates are also higher with the concomitant greater concentrations of initiator. Polymer−polymer coupling reactions are facilitated at low molar mass. Moreover, characterization of low molar mass block polymers is easier using techniques like NMR spectroscopy and mass spectrometry. In addition, high degrees of incompatibility may facilitate block polymer purification, for example, separation of homopolymer impurities using selective solvents. The drive to lower and lower molar masses makes feasible the preparation of precisely monodisperse block polymers, although this is accompanied by the loss of continuous control over composition due to the discrete nature of N. Smaller domains contain fewer polymer chains, hence dispersity must be accompanied by a distribution of feature sizes (i.e., with a statistical distribution of chains per domain) when $Đ > 1$. How detailed molar mass and composition distribution affects pattern fidelity in the low N limit remains an important open question.

Whether these materials are actually useful in practice will be determined by myriad other factors, including control of defect density[74] and application of appropriate metrology techniques,[75] mechanical stability of the polymer features at such length scales, feasibility of pattern transfer and the economic integration of the required processing operations into existing and planned fabrication facilities. Among these difficulties, the most challenging limitation to address may be the technical issues associated with pattern transfer using conventional etching processes. With domain sizes reaching the sub-10 nm scale, dry plasma etching becomes extremely challenging[76] due to strong aspect ratio dependent etching phenomena that considerably limit the efficiency of etching in such confined environments. Recent successes notwithstanding,[77,78] this will generally require new approaches to create arrays of ultrasmall features with controlled shape from self-assembled block polymer templates. Specific inclusion of inorganic precursors in preformed block-polymer systems followed by the elimination of the polymer scaffold presents attractive opportunities. This has been already successfully performed on templates formed from the self-assembly of moderately incompatible block polymers composed of a hydrophobic PS block paired with a more polar block such as PVP[79] or PEO,[51,80] enabling the formation of a great variety of metal oxide particles within the sub-20 nm size range. In our opinion, the elaboration of polymers combining highly incompatible low molar mass blocks, exhibiting a marked hydrophobicity on one hand and hydro(metallo)philicity on the other hand, would enable the facile formation of ultrasmall metal-oxide particles in the sub-5 nm range. This was illustrated in a very recent work,[81] where Schulze et al. were able to prepare 6 nm inorganic particles using PCHE-*b*-PEO block polymer. We see no limitation to achieve small highly incompatible blocks required to achieve these goals. However, the realization of patterning applications with high χ−low N materials will require meeting many materials science and engineering challenges.

■ AUTHOR INFORMATION

Corresponding Authors

*E-mail: christophe.sinturel@univ-orleans.fr.
*E-mail: bates001@umn.edu.
*E-mail: hillmyer@umn.edu.

Notes

The authors declare no competing financial interest.

■ ACKNOWLEDGMENTS

C.S. thanks the University of Minnesota for partial support during his sabbatical leave. CNRS and the Université d'Orléans are acknowledged for support. F.S.B. and M.A.H. were supported primarily by the National Science Foundation through the University of Minnesota MRSEC under Award Number DMR-1420013. We are grateful to Thomas P. Russell, Christopher M. Bates, and Morgan W. Schulze for providing very helpful critical reviews of this manuscript prior to submission.

■ REFERENCES

(1) Markoff, J. IBM Discloses Working Version of a Much Higher-Capacity Chip. *The New York Times*; The New York Times Company: New York, July 9 2015; p B2.
(2) http://www.itrs.net/.
(3) Morris, M. A. *Microelectron. Eng.* **2015**, *132*, 207−217.
(4) Bates, C. M.; Maher, M. J.; Janes, D. W.; Ellison, C. J.; Willson, C. G. *Macromolecules* **2014**, *47*, 2−12.
(5) Koo, K.; Ahn, H.; Kim, S.-W.; Ryu, D. Y.; Russell, T. P. *Soft Matter* **2013**, *9*, 9059−9071.
(6) Luo, M.; Epps, T. H., III *Macromolecules* **2013**, *46*, 7567−7579.
(7) Nunns, A.; Gwyther, J.; Manners, I. *Polymer* **2013**, *54*, 1269−1284.
(8) Jeong, S.-J.; Kim, J. Y.; Kim, B. H.; Moon, H.-S.; Kim, S. O. *Mater. Today* **2013**, *16*, 468−476.
(9) Hiemenz, P. C.; Lodge, T. P. *Polymer Chemistry*, 2nd ed.; CRC Press, Taylor & Francis Group: Boca Raton, FL, U.S.A., 2007.
(10) Leibler, L. *Macromolecules* **1980**, *13*, 1602−1617.
(11) Bates, F. S.; Fredrickson, G. H. *Annu. Rev. Phys. Chem.* **1990**, *41*, 525−557.
(12) Bates, F. S.; Fredrickson, G. H. *Phys. Today* **1999**, *52*, 32−38.
(13) Bang, J.; Jeong, U.; Ryu, D. Y.; Russell, T. P.; Hawker, C. J. *Adv. Mater.* **2009**, *21*, 4769−4792.
(14) Kim, S. H.; Misner, M. J.; Xu, T.; Kimura, M.; Russell, T. P. *Adv. Mater.* **2004**, *16*, 226−231.
(15) Jung, Y. S.; Ross, C. A. *Nano Lett.* **2007**, *7*, 2046−2050.
(16) Bang, J.; Kim, S. H.; Drockenmuller, E.; Misner, M. J.; Russell, T. P.; Hawker, C. J. *J. Am. Chem. Soc.* **2006**, *128*, 7622−7629.
(17) Cavicchi, K. A.; Russell, T. P. *Macromolecules* **2007**, *40*, 1181−1186.

(18) Park, S.-M.; Park, O.-H.; Cheng, J. Y.; Rettner, C. T.; Kim, H.-C. *Nanotechnology* **2008**, *19*, 455304.
(19) Ruzette, A. V. G.; Soo, P. P.; Sadoway, D. R.; Mayes, A. M. *J. Electrochem. Soc.* **2001**, *148*, A537−A543.
(20) Epps, T. H., III; Bailey, T. S.; Pham, H. D.; Bates, F. S. *Chem. Mater.* **2002**, *14*, 1706−1714.
(21) Park, S.; Lee, D. H.; Xu, J.; Kim, B.; Hong, S. W.; Jeong, U.; Xu, T.; Russell, T. P. *Science* **2009**, *323*, 1030−1033.
(22) Nunns, A.; Gwyther, J.; Manners, I. *Polymer* **2013**, *54*, 1269−1284.
(23) Hartney, M. A.; Novembre, A. E.; Bates, F. S. *J. Vac. Sci. Technol., B: Microelectron. Process. Phenom.* **1985**, *3*, 1346−1351.
(24) Jung, Y. S.; Chang, J. B.; Verploegen, E.; Berggren, K. K.; Ross, C. A. *Nano Lett.* **2010**, *10*, 1000−1005.
(25) Jeong, J. W.; Park, W. I.; Kim, M.-J.; Ross, C. A.; Jung, Y. S. *Nano Lett.* **2011**, *11*, 4095−4101.
(26) Luo, Y.; Montarnal, D.; Kim, S.; Shi, W.; Barteau, K. P.; Pester, C. W.; Hustad, P. D.; Christianson, M. D.; Fredrickson, G. H.; Kramer, E. J.; Hawker, C. J. *Macromolecules* **2015**, *48*, 3422−3430.
(27) Rodwogin, M. D.; Spanjers, C. S.; Leighton, C.; Hillmyer, M. A. *ACS Nano* **2010**, *4*, 725−732.
(28) Pitet, L. M.; Wuister, S. F.; Peeters, E.; Kramer, E. J.; Hawker, C. J.; Meijer, E. W. *Macromolecules* **2013**, *46*, 8289−8295.
(29) Bates, C. M.; Seshimo, T.; Maher, M. J.; Durand, W. J.; Cushen, J. D.; Dean, L. M.; Blachut, G.; Ellison, C. J.; Willson, C. G. *Science* **2012**, *338*, 775−779.
(30) Durand, W. J.; Blachut, G.; Maher, M. J.; Sirard, S.; Tein, S.; Carlson, M. C.; Asano, Y.; Zhou, S. X.; Lane, A. P.; Bates, C. M.; Ellison, C. J.; Willson, C. G. *J. Polym. Sci., Part A: Polym. Chem.* **2015**, *53*, 344−352.
(31) Maher, M. J.; Bates, C. M.; Blachut, G.; Sirard, S.; Self, J. L.; Carlson, M. C.; Dean, L. M.; Cushen, J. D.; Durand, W. J.; Hayes, C. O.; Ellison, C. J.; Willson, C. G. *Chem. Mater.* **2014**, *26*, 1471−1479.
(32) Maher, M. J.; Rettner, C. T.; Bates, C. M.; Blachut, G.; Carlson, M. C.; Durand, W. J.; Ellison, C. J.; Sanders, D. P.; Cheng, J. Y.; Willson, C. G. *ACS Appl. Mater. Interfaces* **2015**, *7*, 3323−3328.
(33) Cushen, J. D.; Bates, C. M.; Rausch, E. L.; Dean, L. M.; Zhou, S. X.; Willson, C. G.; Ellison, C. J. *Macromolecules* **2012**, *45*, 8722−8728.
(34) Cushen, J. D.; Otsuka, I.; Bates, C. M.; Halila, S.; Fort, S.; Rochas, C.; Easley, J. A.; Rausch, E. L.; Thio, A.; Borsali, R.; Willson, C. G.; Ellison, C. J. *ACS Nano* **2012**, *6*, 3424−3433.
(35) Aissou, K.; Otsuka, I.; Rochas, C.; Fort, S.; Halila, S.; Borsali, R. *Langmuir* **2011**, *27*, 4098−4103.
(36) Zha, W.; Han, C. D.; Lee, D. H.; Han, S. H.; Kim, J. K.; Kang, J. H.; Park, C. *Macromolecules* **2007**, *40*, 2109−2119.
(37) Chaudhari, A.; Ghoshal, T.; Shaw, M. T.; Cummins, C.; Borah, D.; Holmes, J. D.; Morris, M. A. *Proc. SPIE* **2014**, *9051*, 905110.
(38) Kennemur, J. G.; Hillmyer, M. A.; Bates, F. S. *Macromolecules* **2012**, *45*, 7228−7236.
(39) Sweat, D. P.; Kim, M.; Larson, S. R.; Choi, J. W.; Choo, Y.; Osuji, C. O.; Gopalan, P. *Macromolecules* **2014**, *47*, 6687−6696.
(40) Kennemur, J. G.; Yao, L.; Bates, F. S.; Hillmyer, M. A. *Macromolecules* **2014**, *47*, 1411−1418.
(41) Helfand, E.; Wasserman, Z. R. *Macromolecules* **1976**, *9*, 879−888.
(42) Helfand, E.; Wasserman, Z. R. *Macromolecules* **1978**, *11*, 960−966.
(43) Helfand, E.; Wasserman, Z. R. *Macromolecules* **1980**, *13*, 994−998.
(44) Fredrickson, G. H.; Helfand, E. *J. Chem. Phys.* **1987**, *87*, 697−705.
(45) Park, S.-M.; Liang, X.; Harteneck, B. D.; Pick, T. E.; Hiroshiba, N.; Wu, Y.; Helms, B. A.; Olynick, D. L. *ACS Nano* **2011**, *5*, 8523−8531.
(46) Andersen, T. H.; Tougaard, S.; Larsen, N. B.; Almdal, K.; Johannsen, I. *J. Electron Spectrosc. Relat. Phenom.* **2001**, *121*, 93−110.
(47) Baruth, A.; Seo, M.; Lin, C. H.; Walster, K.; Shankar, A.; Hillmyer, M. A.; Leighton, C. *ACS Appl. Mater. Interfaces* **2014**, *6*, 13770−13781.
(48) Zalusky, A. S.; Olayo-Valles, R.; Wolf, J. H.; Hillmyer, M. A. *J. Am. Chem. Soc.* **2002**, *124*, 12761−12773.
(49) Xu, T.; Kim, H.-C.; DeRouchey, J.; Seney, C.; Levesque, C.; Martin, P.; Stafford, C. M.; Russell, T. P. *Polymer* **2001**, *42*, 9091−9095.
(50) Russell, T. P.; Hjelm, R. P.; Seeger, P. A. *Macromolecules* **1990**, *23*, 890−893.
(51) Mayeda, M. K.; Hayat, J.; Epps, T. H.; Lauterbach, J. *J. Mater. Chem. A* **2015**, *3*, 7822−7829.
(52) Cochran, E. W.; Morse, D. C.; Bates, F. S. *Macromolecules* **2003**, *36*, 782−792.
(53) Glaser, J.; Medapuram, P.; Beardsley, M. W.; Matsen, M. W.; Morse, D. C. *Phys. Rev. Lett.* **2014**, *113*, 068302.
(54) Medapuram, P.; Glaser, J.; Morse, D. C. *Macromolecules* **2015**, *48*, 819−839.
(55) Kim, S.; Nealey, P. F.; Bates, F. S. *Nano Lett.* **2014**, *14*, 148−152.
(56) Wan, L.; Ruiz, R.; Gao, H.; Patel, K. C.; Albrecht, T. R.; Yin, J.; Kim, J.; Cao, Y.; Lin, G. *ACS Nano* **2015**, *9*, 7506−7514.
(57) Mishra, V.; Fredrickson, G. H.; Kramer, E. J. *ACS Nano* **2012**, *6*, 2629−2641.
(58) Marencic, A. P.; Register, R. A. *Annu. Rev. Chem. Biomol. Eng.* **2010**, *1*, 277−297.
(59) Li, W.; Nealey, P. F.; de Pablo, J. J.; Muller, M. *Phys. Rev. Lett.* **2014**, *113*, 168301.
(60) Sinturel, C.; Vayer, M.; Morris, M.; Hillmyer, M. A. *Macromolecules* **2013**, *46*, 5399−5415.
(61) Lodge, T. P.; Pudil, B.; Hanley, K. J. *Macromolecules* **2002**, *35*, 4707−4717.
(62) Fredrickson, G. H.; Leibler, L. *Macromolecules* **1989**, *22*, 1238−1250.
(63) Peters, A. J.; Lawson, R. A.; Nation, B. D.; Ludovice, P. J.; Henderson, C. L. *Proc. SPIE* **2014**, *9049*, 90492.
(64) Rosedale, J. H.; Bates, F. S. *Macromolecules* **1990**, *23*, 2329−2338.
(65) Zhao, Y.; Sivaniah, E.; Hashimoto, T. *Macromolecules* **2008**, *41*, 9948−9951.
(66) Kim, J. K.; Lee, H. H.; Gu, Q.-J.; Chang, T.; Jeong, Y. H. *Macromolecules* **1998**, *31*, 4045−4048.
(67) Lee, S.; Gillard, T. M.; Bates, F. S. *AIChE J.* **2013**, *59*, 3502−3513.
(68) Voronov, V. P.; Buleiko, V. M.; Podneks, V. E.; Hamley, I. W.; Fairclough, J. P. A.; Ryan, A. J.; Mai, S.-M.; Liao, B.-X.; Booth, C. *Macromolecules* **1997**, *30*, 6674−6676.
(69) Gilliard, T. M.; Phelan, D.; Leighton, C.; Bates, F. S. *Macromolecules* **2015**, *48*, 4733−4741.
(70) Broer, D. J.; Bastiaansen, C. M. W.; Debije, M. G.; Schenning, A. P. H. J. *Angew. Chem., Int. Ed.* **2012**, *51*, 7102−7109.
(71) Gin, D. L.; Noble, R. D. *Science* **2011**, *332*, 674−676.
(72) Luckhurst, G. R.; Zannoni, C. *Nature* **1977**, *267*, 412−414.
(73) Feng, X.; Tousley, M. E.; Cowan, M. G.; Wiesenauer, B. R.; Nejati, S.; Choo, Y.; Noble, R. D.; Elimelech, M.; Gin, D. L.; Osuji, C. O. *ACS Nano* **2014**, *8*, 11977−11986.
(74) Simão, C.; Khunsin, W.; Kehagias, N.; Salaun, M.; Zelsmann, M.; Morris, M. A.; Sotomayor, C. M. *Nanotechnology* **2014**, *25*, 175703.
(75) Van Look, L.; Delgadillo, P. R.; Lee, Y.-T.; Pollentier, I.; Gronheid, R.; Cao, Y.; Lin, G.; Nealey, P. F. *Microelectron. Eng.* **2014**, *123*, 175−179.
(76) Borah, D.; Shaw, M. T.; Rasappa, S.; Farrell, R. A.; O'Mahony, C.; Faulkner, C. M.; Bosea, M.; Gleeson, P.; Holmes, J. D.; Morris, M. A. *J. Phys. D: Appl. Phys.* **2011**, *44*, 174012.
(77) Cushen, J.; Wan, L.; Blachut, G.; Maher, M. J.; Albrecht, T. R.; Ellison, C. J.; Willson, C. G. *ACS Appl. Mater. Interfaces* **2015**, *7*, 13476−13483.
(78) Hirahara, E.; Paunescu, M.; Polishchuk, O.; Jeong, E.; Ng, E.; Shan, J.; Kim, J.; Hong, S.; Baskaran, D.; Lin, G.; Vora, A.; Tjio, M.; Arellano, N.; Rettner, C. T.; Lofano, E.; Liu, C.-C.; Tsai, H.; Chunder,

DOI: 10.1021/acsmacrolett.5b00472
ACS Macro Lett. 2015, 4, 1044−1050

A.; Nguyen, K.; Friz, A. M.; Bowers, A. N.; Balakrishnan, S.; Cheng, J. Y.; Sanders, D. P. *Proc. SPIE* **2015**, *9425*, 94250.
(79) Roulet, M.; Vayer, M.; Sinturel, C. *Eur. Polym. J.* **2013**, *49*, 3897−3903.
(80) Ghoshal, T.; Maity, T.; Godsell, J. F.; Roy, S.; Morris, M. A. *Adv. Mater.* **2012**, *24*, 2390−2397.
(81) Schulze, , M. W.; Sinturel, , C.; Hillmyer, , M. A. *ACS Macro Lett.* **2015**, *4*, 1027−1032.

DOI: 10.1021/acsmacrolett.5b00472
ACS Macro Lett. 2015, 4, 1044−1050